Numerical Modeling of Pressurization of a Propellant Tank

Alok Majumdar* and Todd Steadman†
Sverdrup Technology Huntsville, Alabama 35806

An unsteady finite volume procedure has been developed to predict the history of pressure, temperature, and mass flow rate of the pressurant and propellant during the expulsion of the propellant from a tank. The time-dependent mass, momentum, entropy, and fluid specie conservation equations are solved at the ullage space. The model accounts for the change in the ullage volume due to expulsion of the propellant. It also accounts for the heat transfer from the ullage gas to the tank wall and propellant and the mass transfer from the propellant to the ullage gas. The predicted pressure and temperature of the ullage, the temperature of the tank wall, and the pressurant flow rates into the tank during pressurization have been presented for a simple test case. The results of several test cases were compared with a published correlation of pressurant requirements for a given displacement of propellant. The agreement between the predictions and the correlation was found to be satisfactory. Inclusion of mass transfer, in general, improved the comparison between the numerical prediction and the published correlation.

Nomenclature

A	=	area, ft^2
A_{sw}	=	surface area swept by liquid free surface during expulsion, ft^2
C	=	ratio of wall to gas effective thermal capacity
c	=	mass concentration
c_p	=	constant pressure specific heat, $\mathrm{Btu/lbm \cdot R}$
D_{eq}	=	equivalent tank diameter, ft
Gr	=	Grashof number
g	=	gravitational acceleration, $\mathrm{ft/s}^2$
g_c	=	conversion constant ($32.174\ \mathrm{lbm \cdot ft/lbf \cdot s}^2$)
H	=	propellant height, ft
h	=	enthalpy, Btu/lbm
h_c	=	heat transfer coefficient, $\mathrm{Btu/s \cdot ft^2 \cdot R}$
J	=	mechanical equivalent of heat ($778\ \mathrm{ft \cdot lbf/Btu}$)
K_f	=	flow resistance coefficient, $\mathrm{lbf \cdot s^2/(lbm \cdot ft)^2}$
K_H	=	heat transfer factor
k	=	conductivity, $\mathrm{Btu/s \cdot ft \cdot R}$
l_S	=	length scale, ft
m	=	resident mass, lbm
m_{wall}	=	tank wall mass, lbm
$\dot{m}$	=	mass flow rate, lbm/s
Pr	=	Prandtl number
p	=	pressure, $\mathrm{lbf/ft}^2$
$p_1 - p_8$	=	constants of Epstein and Anderson's correlation[2]
Q	=	ratio of total ambient heat input to effective thermal capacitance of gas
Q_i	=	heat source, Btu/s
$\dot{Q}$	=	heat transfer rate, Btu/s
$\dot{q}$	=	ambient heat flux, Btu/s
S	=	modified Stanton number
$\dot{S}_{gen}$	=	entropy generation, $\mathrm{Btu/s \cdot R}$
s	=	entropy, $\mathrm{Btu/lbm \cdot R}$
T	=	temperature, R
u	=	velocity, ft/s
V	=	volume, ft^3
v	=	specific volume, ft^3
w_p	=	pressurant mass, lbm
β	=	coefficient of thermal expansion, 1/R
ΔT	=	temperature difference, R
ΔV	=	expelled liquid volume, ft^3
δ_{wall}	=	tank wall thickness, ft
θ	=	angle between branch flow velocity vector and gravity vector, deg
θ_T	=	total liquid outflow time, s
μ	=	viscosity, $\mathrm{lbm/ft \cdot s}$
ρ	=	density, $\mathrm{lbm/ft}^3$

*Engineering Specialist, Space Transportation Directorate, 620 Discovery Drive; currently Aerospace Technologist, Thermodynamics and Heat Transfer Group, ED25 National Aeronautics and Space Administration, Marshall Space Flight Center, Huntsville, Alabama 35812. Member AIAA.
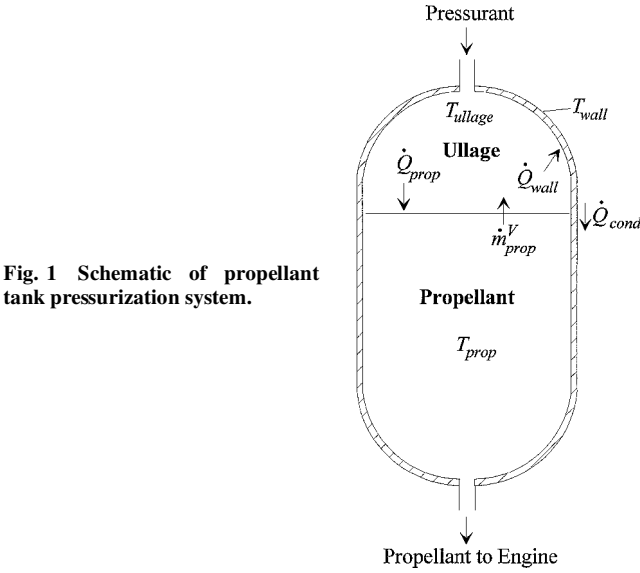†Engineer, Space Transportation Directorate, 620 Discovery Drive. Member AIAA.

Introduction

THE purpose of the pressurization system is to control the pressure in the gas space of the propellant tank (known as the ullage space) and the propellant mass flow rate to the engine. A mathematical model is required to predict the ullage and propellant conditions to ensure that pressure and temperature levels inside the tank remain within acceptable limits and that the propellant pressure leaving the tank satisfies the net positive suction pressure (NPSP) requirement of the pump feeding the engine. The pressurization of a propellant tank is a complex thermodynamic process with heat and mass transfer in a stratified environment. Ring[1] described the physical processes and heat transfer correlation in his monograph. Epstein and Anderson[2] developed an equation for the prediction of cryogenic pressurant requirements for axisymmetric propellant tanks. Recently, Van Dresar[3] improved the accuracy of Epstein and Anderson's correlation[2] for liquid hydrogen tanks. However, a general purpose computer program that could model flow distribution in the pressurant supply line, pressurization, heat transfer, and mass transfer in the ullage volume and propellant flow conditions to the engine was not available. In this paper, we describe a finite volume procedure to model pressurization, heat transfer, and mass transfer in a propellant tank. This procedure was subsequently implemented in a general-purpose computer program to predict fluid and thermodynamic parameters during the pressurization process.

A schematic of the considered propellant tank pressurization system is shown in Fig. 1. It is assumed that initially the ullage space is filled with pressurant at the propellant temperature. As warm pressurant enters the ullage space, it mixes with the cold pressurant already present and the temperature of the ullage begins to increase due to mixing and compression. Initially, the walls of the tank are at propellant temperature as well. Heat transfer from the ullage gas to the propellant and the tank wall and mass transfer from the propellant to the ullage start taking place immediately after the pressurant begins flowing into the tank. Propellant flows from the tank to the

Fig. 1 Schematic of propellant tank pressurization system.

Fig. 2 Schematic of numerical model nodes, branches, and indexing practice.

Fig. 3 Schematic of a branch showing gravity.

engine under the influence of ullage pressure and gravitational head in the tank.

The finite volume procedure described in this paper models the following physical processes: 1) change in ullage and propellant volume, 2) change in gravitational head in the tank, 3) heat transfer from ullage to propellant, 4) heat transfer from ullage to the tank wall, 5) heat conduction between the ullage exposed tank surface and the propellant exposed tank surface, and 6) mass transfer from propellant to ullage.

Governing Equations

Numerical modeling of a pressurization process requires the solution of unsteady mass, momentum, entropy, and fluid specie conservation equations in conjunction with thermodynamic equations of state. The mass, momentum, entropy, and fluid specie equations are first expressed in a finite volume form in an unstructured system of coordinates as shown in Figs. 2 and 3. Figure 2 displays a schematic showing adjacent nodes, their connecting branches, and the indexing system used by the numerical model. A schematic showing a branch with upstream and downstream nodes is shown in Fig. 3. To solve for the unknown variables, mass, entropy, and fluid specie conservation equations are written for each internal node, and flow rate equations are written for each branch.

Mass Conservation Equation

The mass conservation equation is

$$\frac{m_{\tau + \Delta\tau} m_{\tau}}{\Delta\tau} = \sum_{j=1}^{j=n} \dot{m}_{ij} + \dot{m}_{i,\text{source}} \tag{1}$$

Equation (1) requires that the net mass flow from a given node i, shown in Fig. 2, must equate to the rate of change of mass in the control volume. The mass transfer from propellant to ullage is represented by the external mass source term $\dot{m}_{i,\text{source}}$.

Momentum Conservation Equation

The flow rate in a branch is calculated from the momentum conservation equation [Eq. (2)], which represents the balance of fluid forces acting on a given branch (Fig. 3). This formulation can model several kinds of fluid forces as shown in Eq. (2):

$$\frac{(m_{u_{\tau+\Delta\tau}} - m_{u_{\tau}})}{g_c \Delta\tau} + \frac{\dot{m}_{ij}}{g_c}(u_{ij} - u_u) = (p_i - p_j)A$$

$$+ \frac{\rho g V \cos\theta}{g_c} - K_f \dot{m}_{ij}|\dot{m}_{ij}|A \tag{2}$$

The two terms in the left-hand side of the momentum equation represent the inertia of the fluid. The first one is the time-dependent term and must be considered for unsteady calculations. The second
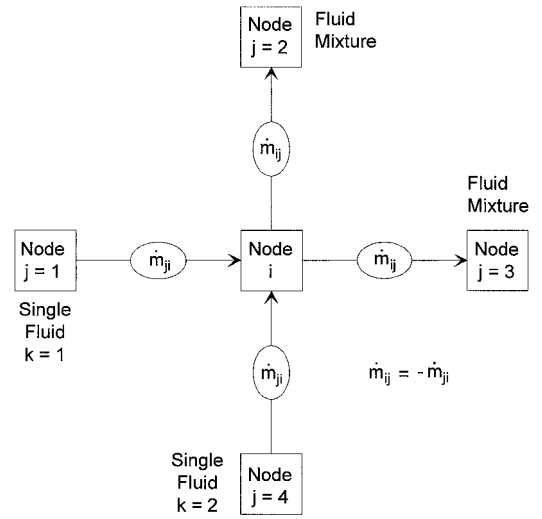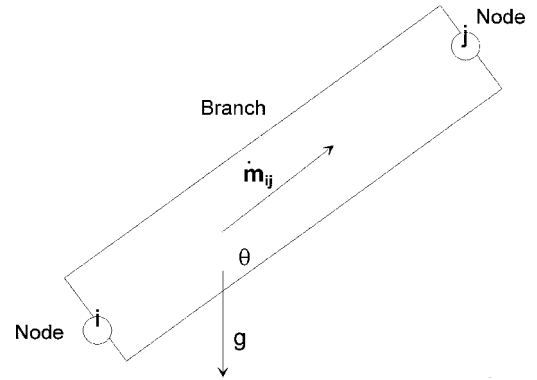
term is significant when there is a large change in area or density from branch to branch. The first term in the right-hand side of the momentum equation represents the pressure gradient in the branch. The pressures are located at the upstream and downstream face of a branch. The second term represents the effect of gravity. The gravity vector makes an angle θ with the assumed flow direction vector. The third term represents the frictional effect. Friction was modeled as a product of K_f and the square of the flow rate and area. K_f is a function of the fluid density in the branch and the nature of the flow passage being modeled by the branch.

Note that the inertia and gravitational terms in Eq. (2) are not required for modeling pressurization and were not considered in Eq. (2). Instead, the gravitational effect was accounted for by calculating pressure at the ullage and propellant interface as shown in Eq. (9).

Entropy Conservation Equation

The entropy conservation equation for node i, shown in Fig. 2, can be expressed mathematically as shown in Eq. (3a):

$$\frac{(m_i s_i)_{\tau + \Delta\tau} - (m_i s_i)_{\tau}}{\Delta\tau} = \sum_{j=1}^{j=n} \{\max[-\dot{m}_{ij}, 0]s_j - \max[\dot{m}_{ij}, 0]s_i\}$$

$$+ \sum_{j=1}^{j=n} \left\{ \frac{\max[-\dot{m}_{ij}, 0]}{|\dot{m}_{ij}|} \right\} \dot{S}_{ij,\text{gen}} + \frac{Q_i}{T_i} \tag{3a}$$

The entropy generation rate due to fluid friction in a branch is expressed by Eq. (3b)

$$\dot{S}_{ij,\text{gen}} = \frac{\dot{m}_{ij}\Delta p_{ij,\text{viscous}}}{\rho_u T_u J} = \frac{K_f(|\dot{m}_{ij}|)^3}{\rho_u T_u J} \tag{3b}$$

Equation (3a) shows that for unsteady flow, the rate of increase of entropy in the control volume is equal to the rate of entropy

transport into the control volume plus the rate of entropy generation in all upstream branches due to fluid friction, plus the rate of entropy added to the control volume due to heat transfer. The max operator in Eq. (3) reflects the use of an upwind differencing scheme that has been extensively employed in the numerical solution of Navier–Stokes equations in convection heat transfer and fluid flow applications. When the flow direction is not known, this operator allows the transport of entropy only from its upstream neighbor. In other words, the upstream neighbor influences its downstream neighbor but not vice versa. The first term in the right-hand side of the equation represents the advective transport of entropy from neighboring nodes. The second term represents the rate of entropy generation in branches connected to the ith node. The third term represents entropy change due to heat transfer.

Fluid Specie Conservation Equation

$$\frac{(m_i c_{i,k})_{\tau+\Delta\tau} - (m_i c_{i,k})_\tau}{\Delta\tau} = \sum_{j=1}^{j=n} \{\max[-\dot{m}_{ij}, 0]\, c_{j,k}$$

$$- \max[\dot{m}_{ij}, 0]\, c_{i,k}\} + S_{i,k} \qquad (4)$$

Equation (4) requires that the rate of increase of the concentration of the kth specie in the given node i, shown in Fig. 2, equals the rate of transport of the kth specie into the control volume minus the rate of transport of the kth specie out of the control volume. $S_{i,k}$ represents the source term for the kth specie in the ith node.

The physical processes observed in a tank pressurization system are expressed mathematically hereafter.

Change in Ullage and Propellant Volume

Because of the discharge of propellant to the engine, resident propellant volume decreases and, subsequently, ullage volume increases.

$$dV_{\text{ullage}} = \frac{\dot{m}_{\text{prop}}\Delta\tau}{\rho_{\text{prop}}} = -dV_{\text{prop}} \qquad (5)$$

At all times the following geometric condition is satisfied:

$$V_{\text{ullage}} + V_{\text{prop}} = V_{\text{tank}} \qquad (6)$$

At each time step, propellant and ullage volumes are calculated from the following relations:

$$V_{\text{prop}}^{\tau+\delta\tau} = V_{\text{prop}}^{\tau} - dV_{\text{prop}} \qquad (7)$$

$$V_{\text{ullage}}^{\tau+\delta\tau} = V_{\text{ullage}}^{\tau} + dV_{\text{ullage}}^{\tau+\delta\tau} \qquad (8)$$

Change in Gravitational Head in the Tank

With the change in the propellant volume, the gravitational head H in the tank decreases. The pressure at the tank bottom is calculated from the following relation:

$$p_{\text{tank bottom}} = p_{\text{ullage}} + (\rho_{\text{prop}}gH)/g_c \qquad (9)$$

Heat Transfer from Ullage Gas to Propellant

The heat transfer from the ullage gas to the propellant is expressed as

$$\dot{Q}_{\text{prop}} = [h_c A]_{\text{ullage}-\text{prop}}(T_{\text{ullage}} - T_{\text{prop}}) \qquad (10)$$

It has been assumed that the heat transfer is due to natural convection with the heat transfer coefficient expressed as

$$h_c = K_H C (k_f/l_s) X^n \qquad (11)$$

where,

$$X = (Gr)(Pr) \qquad (12)$$

$$Gr = \left(l_s^3 \rho_f^2 g \beta_f |\Delta T| / \mu_f^2\right) \qquad (13)$$

$$Pr = c_{pf} \mu_f / k_f \qquad (14)$$

Gr and Pr are the Grashof number and the Prandtl number of the ullage gas, respectively.

According to Ring,[1] $C = 0.27$, $n = 0.25$, and K_H (heat transfer adjustment factor) is set to 1.0. The length scale in Eq. (13) is set to the diameter of the tank.

Heat Transfer from Ullage Gas to Wall

The heat transfer from the ullage gas to the wall is expressed as

$$\dot{Q}_{\text{wall}} = [h_c A]_{\text{ullage}-\text{wall}}(T_{\text{ullage}} - T_{\text{wall}}) \qquad (15)$$

It has also been assumed that the heat transfer is due to natural convection and the heat transfer coefficient is expressed by Eqs. (11–14). According to Ring,[1] $C = 0.54$ and $n = 0.25$ for this case. The diameter of the tank was again considered to be the length scale used in the heat transfer correlation.

Transient Heat Transfer in the Tank

Wall temperature has been calculated from a transient heat conduction equation:

$$m_{\text{wall}} c_{p,\text{wall}} \frac{\partial T_{\text{wall}}}{\partial\tau} = \dot{Q}_{\text{wall}} - \dot{Q}_{\text{cond}} \qquad (16)$$

where

$$m_{\text{wall}} = \rho_{\text{wall}} A_{\text{ullage to wall}} \delta_{\text{wall}} \qquad (17)$$

$$\dot{Q}_{\text{cond}} = k_{\text{tank}} A_{\text{cond}} (T_{\text{wall}} - T_{\text{prop}})/(H/2) \qquad (18)$$

The model accounts for the change in the heat transfer area as the ullage volume increases during the pressurization process. However, the area was calculated assuming a cylindrically shaped tank. The tank diameter has been assumed to be the length scale in both heat transfer correlations [Eqs. (10) and (15)].

Mass Transfer from Propellant to Ullage Gas

The mass transfer rate from the propellant to the ullage gas is calculated from the heat transfer rate [Eq. (10)]. It is assumed that the propellant is vaporized from the surface and the heat transfer from the ullage only contributes to the vaporization of propellant. The mass transfer due to vaporization is expressed as

$$\dot{m}_{\text{prop}}^{v} = \dot{Q}_{\text{prop}}/[h_{\text{fg}} + c_{\text{pf}}(T_{\text{sat}} - T_{\text{prop}})] \qquad (19)$$

The saturation temperature in Eq. (19) is calculated using the vapor pressure relation

$$\ell n\, p_{\text{sat}} = A + (B/T_{\text{sat}}) + C\,\ell n\, T_{\text{sat}} + D T_{\text{sat}} \qquad (20)$$

where A, B, C, and D are fluid specific vapor pressure relation constants. Table 1 lists the values of the vapor pressure relation constants for the propellants considered in this paper.

The enthalpy of vaporization in Eq. (19) is calculated using the Clapeyron equation:

$$h_{\text{fg}} = T_{\text{sat}}(v_g - v_f) \left.\frac{dP}{dT}\right|_{\text{sat}} \qquad (21)$$

where v_g is found using the Lee and Kesler modified Benedict-Webb-Rubin equation as described by Reid et al.[4] and v_f is determined from the following correlation:

$$v_f = C_0 + C_1 T + C_2 T^2 + C_3 T^3 + \cdots \qquad (22)$$

Table 1   Vapor pressure relation constants

Fluid	A	B	C	D
Oxygen	81.66	−2857.0	−13.05	0.0310
Nitrogen	67.79	−2156.0	−10.97	0.0327
Hydrogen	11.40	−211.9	−1.228	0.0405

Table 2 Liquid specific volume correlation constants

	Oxygen	Nitrogen	Hydrogen
C_0	-0.34614	-0.01204	-13.132
C_1	0.011286	0.00061	1.7962
C_2	-0.00013837	$-4.23216E-06$	-0.094964
C_3	$8.2613E-07$	$1.06765E-08$	0.002464
C_4	$-2.4007E-09$	——	$-3.1377E-05$
C_5	$2.7247E-12$	——	$1.5712E-07$

where C_0, C_1, C_2, etc. are curve fit constants. Table 2 lists the values of the correlation constants for the propellants considered in this paper.

Numerical Model

A pressurization system numerical model was developed to test the implementation of the pressurization option using the Generalized Fluid System Simulation Program (GFSSP).[5,6] The system considered consists of a vertically mounted 71.5-in.-diam cylindrical aluminum tank with a wall thickness of 0.375 in. and a volume of 500 ft³. The pressurant is helium and the propellant is liquid oxygen (LOX). The tank initially contains 475 ft³ of LOX with a 25 ft³ ullage space that is filled with helium at 67 psia and −264°F. Helium at 95 psia and 120°F enters the ullage space through an orifice. LOX exits the bottom of the tank through a restriction and flows to the engine inlet, which has a pressure of 50 psia. The restriction between the tank exit and the engine inlet is set to limit the propellant flow such that the tank is completely drained in 200 s.

Result and Discussion

Figure 4 shows both the ullage pressure and tank bottom pressure histories for the test model. After an initial pressure rise due to a ramping up transient effect, both pressures begin a slow but steady decline for the remainder of the run. Note that tank bottom pressure was calculated [Eq. (9)] by adding ullage pressure with pressure due to gravitational head. Figure 4 shows that as the gravitational head decreases, the ullage and tank bottom pressures slowly converge until all propellant is drained from the tank. The slow decline in ullage pressure is mainly due to the expanding ullage volume.

Figure 5 shows the histories for the ullage temperature and the tank wall temperature. Figure 5 shows that the tank wall temperature rises 34°F over the course of the model run, revealing that the 120°F helium gas entering the tank has an increasing effect on the tank wall as propellant is drained from the tank and the wall surface area exposed to the warmer ullage gas grows. This effect is somewhat dampened, however, because the heat gained by the wall is conducted to the portion of the tank that is submerged in LOX, which acts as a heat sink. The ullage temperature rises 208°F during the first 60 s of tank pressurization before beginning a slow decline for the remainder of the simulation. This large initial temperature rise is primarily due to the mixing of hot helium gas with the relatively cold gas present in the ullage. The decline in temperature is a result of expansion due to continuous increase of the ullage volume.
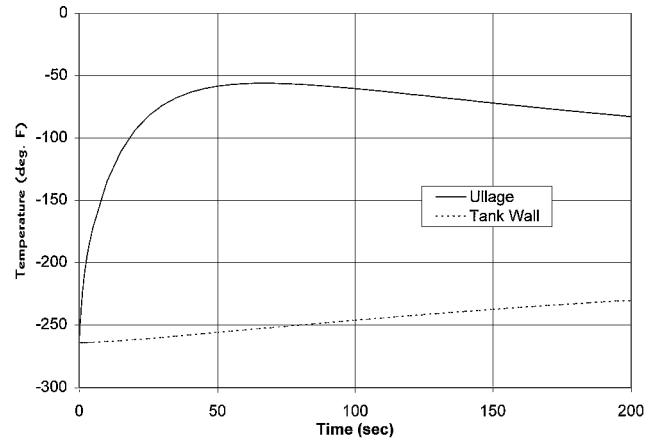
Helium flow rate into the tank is shown in Fig. 6. The helium flow rate was found to drop initially as the start transient takes place, which is consistent with the ramp up effect noted in Fig. 4. Then the flow rate begins to gradually increase as ullage pressure drops due to the expanding ullage volume. The ullage volume increases linearly throughout the run. All 475 ft³ of LOX is discharged from the tank during the pressurization process. The LOX flow rate curve, not shown here, mirrors the ullage and tank bottom pressure curves, rising through an initial start transient to a peak value and then declining for the remainder of the run as tank pressure drops.

Figure 7 shows the mass transfer rate of gaseous oxygen (GOX) into the ullage space over the duration of the run. The mass transfer rate curve mirrors the ullage temperature curve, which is what one expects because the mass transfer is based on the ullage to propellant heat transfer, which is based on ullage temperature.
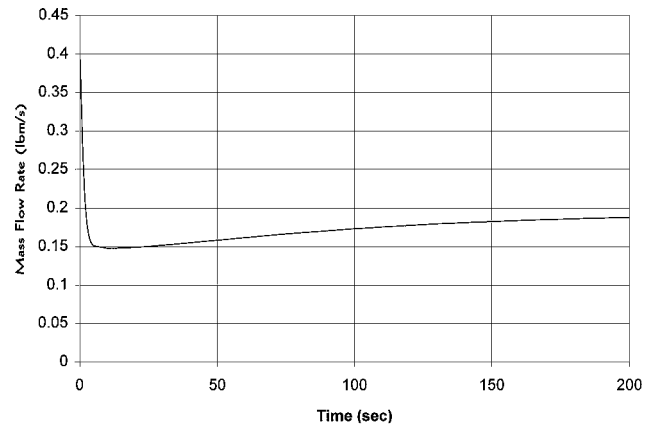
As a validation, finite volume procedure predictions were compared with a published correlation of pressurant requirements for
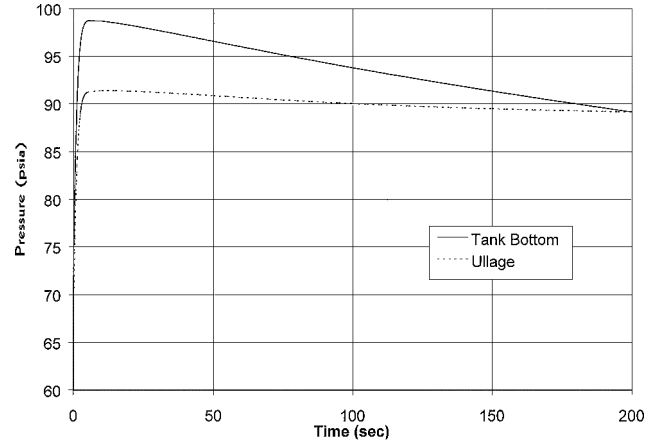
Fig. 4 Ullage and tank bottom pressure history.

Fig. 5 Ullage and tank wall temperature history.

Fig. 6 Helium flow rate into the tank.

a given displacement of propellant as published by Epstein and Anderson.[2] The correlation calculates the collapse factor, which is defined by Van Dresar[3] as a ratio of the actual pressurant consumption to an ideal pressurant consumption where no heat or mass transfer from the pressurant occurs. This correlation takes the form shown in Eqs. (23–27):
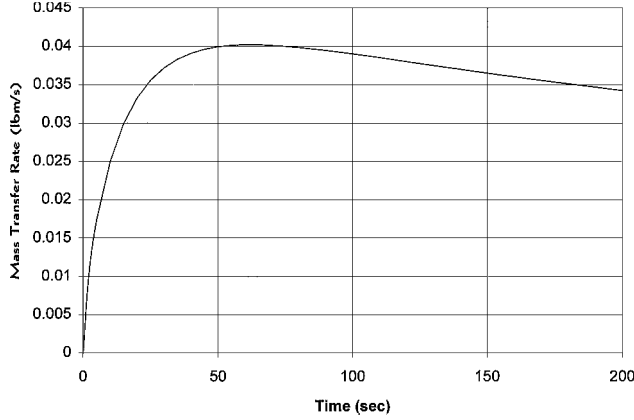
$$w_p / w_p^0 = \left\{ [(T_0/T_s) - 1]\left[1 - \exp\left(-p_1 C^{p_2}\right)\right]\left[1 - \exp\left(-p_3 S^{p_4}\right)\right] \right.$$

$$\left. + 1 \right\} \exp\left\{ -p_5 [1/(1 + C)]^{p_6} [S/(1 + S)]^{p_7} Q^{p_8} \right\} \qquad (23)$$

where

$$w_p^0 = \rho_G^0 \Delta V \qquad (24)$$

Table 3 Pressurization validation results

	Collapse factor			Discrepancy(%)	
Fluid	Epstein and Anderson[2]	GFSSP without mass transfer	GFSSP with mass transfer	Without mass transfer	With mass transfer
Oxygen	1.58	1.35	1.44	14.56	8.86
Hydrogen	1.57	1.42	1.39	9.55	11.46
Nitrogen	1.67	1.37	1.49	17.96	10.78

Fig. 7 GOX mass transfer to ullage.

$$C = \frac{\left(\rho c_p^0 \delta\right)_{\text{wall}}}{(\rho c_p)_G^0 D_{\text{eq}}} \frac{T_s}{T_0} \qquad (25)$$

$$S = \frac{h_c \theta_T}{(\rho c_p)_G^0 D_{\text{eq}}} \frac{T_s}{T_0} \qquad (26)$$

$$Q = \frac{\dot{q}\theta_T}{(\rho c_p)_G^0 D_{\text{eq}} T_0} \qquad (27)$$

Van Dresar[3] later modified this correlation by redefining D_{eq} as shown in Eq. (28):

$$D_{\text{eq}} = 4(\Delta V/A_{\text{sw}}) \qquad (28)$$

The validation exercise consisted of comparing pressurant mass predictions for three different propellants with helium as the pressurant in each case. The three propellants used were oxygen, nitrogen, and hydrogen. Table 3 shows the results of this validation exercise for GFSSP predictions with and without mass transfer. For oxygen and nitrogen, there is a definite improvement in the agreement between GFSSP and Ref. 2 with the addition of mass transfer, reducing nitrogen's prediction discrepancy by 7% and that for oxygen by about 6%. However, the prediction discrepancy for hydrogen actually grows with the addition of mass transfer, increasing by about 2%. The reason for this behavior has to do with the densities of the propellants with respect to the helium pressurant. GOX and nitrogen are more dense than gaseous helium, and so, all other considerations being equal, their presence in the ullage will increase GFSSP's predicted pressurant mass usage for the case with mass transfer, thus increasing the collapse factor and bringing it closer to the Ref. 2 correlation predictions. Hydrogen, on the other hand, is less dense than helium, resulting in a lower pressurant mass prediction in the ullage for the mass transfer case and, thus, a lower collapse factor, increasing the discrepancy between the Ref. 2 correlation and GFSSP.

Several parametric studies were performed to gauge the sensitivity of the pressurization process to parameters such as subcooling, ullage pressure, and heat transfer adjustment factor. These studies showed a more significant influence by the heat transfer adjustment factor than subcooling and ullage pressure. The heat transfer adjustment factor study was performed by varying K_H for the baseline case by ± 0.5.
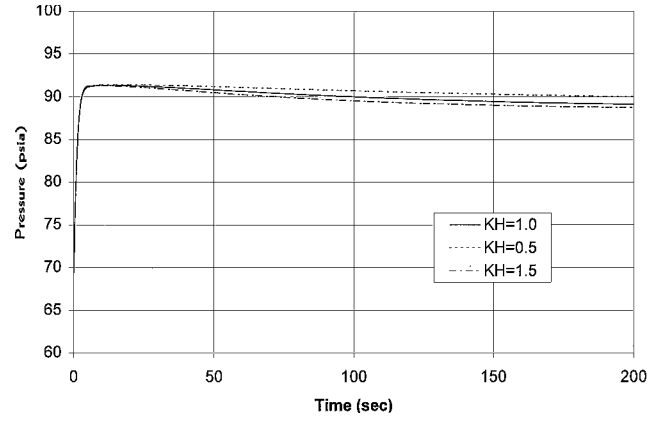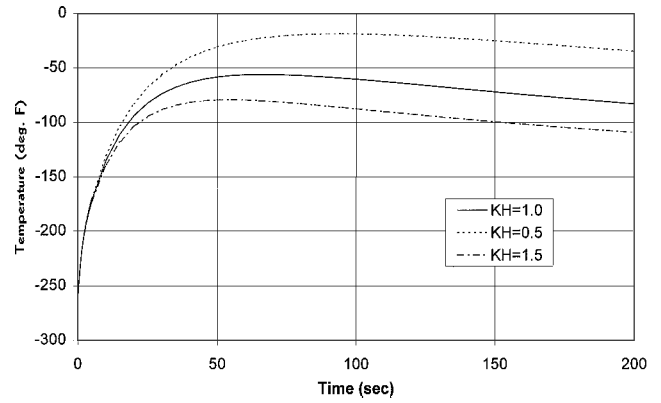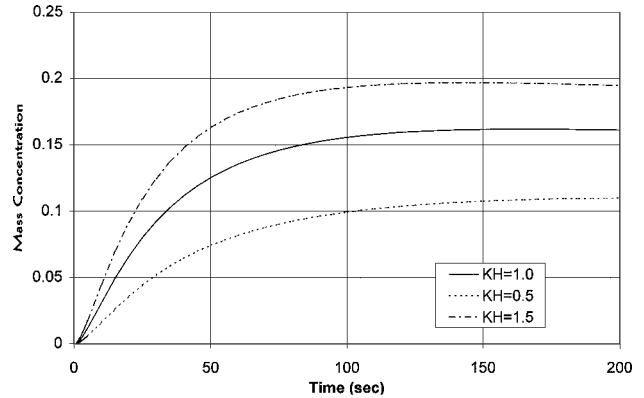

Fig. 8 K_H parametric study ullage pressure comparison.

Fig. 9 K_H parametric study ullage temperature comparison.

Fig. 10 K_H parametric study GOX mass concentration in ullage.

Figure 8 shows a slight effect of K_H on ullage pressure, in which it varies the final predicted ullage pressure from 88.8 to 90 psia. The ullage temperature history is shown in Fig. 9 to be significantly affected by the change in K_H, with final temperature predictions varying over a range of 74°F. As a result, GOX mass concentration in the ullage, which is shown in Fig. 10, also shows a significant variation for changes in K_H, varying from a prediction of 11 to 19.5% GOX by mass in the ullage at the end of the run. It is believed that the sensitivity of the pressurization process to this parameter, which is difficult to calculate accurately, is the major cause of the discrepancy between the Ref. 2 correlation and GFSSP's collapse factor prediction.

Conclusions

A finite volume procedure has been developed to model the pressurization of a propellant tank. A simple model has been developed to test the numerical stability of the algorithm and physical plausibility of the results. The prediction of pressurant requirements compared favorably with the Ref. 2 correlation. Inclusion of mass transfer in the model improves the comparison with the Ref. 2 correlation for propellants heavier than the pressurant. A parametric study on the heat transfer coefficient reveals that uncertainty in the heat transfer coefficient may contribute to the observed discrepancy.

Acknowledgments

References

[1]Ring, E., *Rocket Propellant and Pressurization Systems*, Prentice–Hall, Upper Saddle River, NJ, 1964, pp. 173–245.

[2]Epstein, M., and Anderson, R. E., "An Equation for the Prediction of Cryogenic Pressurant Requirements for Axisymmetric Propellant Tanks," *Advances in Cryogenic Engineering*, Vol. 13, Plenum, New York, 1968, pp. 207–214.

[3]Van Dresar, N. T., "Prediction of Pressurant Mass Requirements for Axisymmetric Liquid Hydrogen Tanks," *Journal of Propulsion and Power*, Vol. 13, No. 6, 1997, pp. 796–799.

[4]Reid, R. C., Prausnitz, J. M., and Poling, B. E., *The Properties of Gases and Liquids*, 4th ed., McGraw–Hill, New York, 1987, p. 47.

[5]Majumdar, A., Bailey, J. W., Schallhorn, P., and Steadman, T., "A Generalized Fluid System Simulation Program to Model Flow Distribution in Fluid Networks," Rept. 331-201-97-005, Sverdrup Technology, Huntsville, AL, 1997.

[6]Majumdar, A., "A Second-Law-Based Unstructured Finite Volume Procedure for Generalized Flow Simulation," AIAA Paper 99-0934, Jan. 1999.